Performance Bounds for Optimum and Suboptimum Reception Under Class-A Impulsive Noise

Jürgen Häring and A. J. Han Vinck, *Senior Member, IEEE*

***Abstract*—The transmission over the memoryless additive white Class-A noise (AWCN) channel is considered. For uncoded transmission, an exact expression for the symbol error rate is derived. For coded transmission, the Chernoff bound on the pairwise error probability is calculated and the performance achieved on the real and the complex AWCN channels is compared. Moreover, a low-complexity, suboptimum decoding metric is derived and analyzed employing the cutoff rate as a performance criterion.**

***Index Terms*—Class-A noise, cutoff rate, impulsive noise, suboptimum reception.**

I. Introduction

In CLASSICAL coding theory, the additive white Gaussian noise (AWGN) channel model is widely applied. It is motivated by the assumption that the transmitted data is corrupted by thermal noise which is present in every real physical receiver. However, in many cases, the transmission is additionally disturbed by man-made noise. Sources for man-made noise are e.g. radio frequency emissions from all sorts of electronic devices, especially if a large number of independent devices is crowded in a small geographical area [13]. The growing number of electronic devices used in all day life, especially wireless communication systems, generate an increasing number of man-made noise environments and makes this noise-type more and more a concern for the design of modern communication systems.

Man-made noise is typically impulsive and therefore not included in the AWGN model. In [7] and [13], it has been reported that transmission systems designed under the AWGN assumption typically suffer from sever performance degradations when exposed to impulsive noise. This shows the need to adapt communication systems to man-made noise.

In [5], Middleton introduced his Class-A, Class-B, and Class-C models for man-made noise. The derivation of the models is based on the mathematical analysis of the physical, noise-generating process (see [1] and [5]). Although the derivation incorporates many simplifications, numerous examples have shown the excellent agreement of the models with measured data from both natural and man-made noise environments. In this paper, the Class-A model is considered. It is distinguished from the Class-B and Class-C models by the assumption that the man-made noise does not cause transients in the receivers RF stages. Due to its simplicity and wide applicability, many authors have considered the Class-A model. In [6] and [16], algorithms to determine the Class-A model's parameters are developed, and in [2] and [4], the model is extended to include antenna-array observations. The Class-A model has also been applied to communications problems. In [13], the performance of binary signaling employing antipodal, orthogonal, and ON–OFF keyed signals is considered. Moreover, the optimum and suboptimum locally optimum Bayes (LOB) detectors are discussed. In [7], the performance of QAM modulation schemes is studied, and [8] addresses trellis-coded modulation under Class-A noise. Furthermore, [9] investigates the impact of Class-A noise on mobile communication systems.

In this paper, we discuss the performance of uncoded and block-coded transmission over the additive white Class-A noise (AWCN) channel. The optimum MAP decoder and a suboptimum receiver with a lower complexity are considered. The choice of a particular system setup is avoided as much as possible to keep the analysis general.

In Section II, the Class-A model is briefly reviewed and the AWCN channel is described using the terminology of communication theory. This nonphysical interpretation gives an intuitive understanding of the Class-A process, and the results presented in this paper naturally follow from this interpretation. Moreover, it motivates a simple algorithm for generating realizations of the Class-A process.

Section III addresses the performance of coded and uncoded transmission when employing MAP decoding. The results mainly extend the investigations given in [13]. Based on the MAP decoding rule discussed in Section III-A, for uncoded transmission, a relation between the symbol error rate (SER) achieved for the AWCN and AWGN channels is derived in III-B. This formula is useful since for the AWGN channel the SERs achieved by most memoryless modulation schemes of practical interest, e.g., ASK, PSK, and QAM, are well known (see [10]). Hence, this result also includes the analysis of QAM modulation given in [7]. A performance analysis of coded transmission is given in Section III-C. It is based on the derivation of the Chernoff upper bound on the pairwise error probability (PEP). The result for the complex AWCN channel is a straightforward extension of the result for the real AWCN channel already given in [13]. However, the comparison of both bounds shows an elementary difference between the real and complex channel.

In Section IV, a suboptimum decoding metric with lower complexity than the MAP metric is derived. A similar metric was applied in [7] and [8] and analyzed using simulation results for a particular coding scheme. Here, a different idea

Paper approved by A. Ahlen, the Editor for Modulation and Signal Design of the IEEE Communications Society. Manuscript received March 15, 2001; revised April 15, 2001 and December 15, 2001.

The authors are with the Institute for Experimental Mathematics, University of Essen, 45326 Essen, Germany (e-mail: haering@exp-math.uni-essen.de; vinck@exp-math.uni-essen.de).

Publisher Item Identifier 10.1109/TCOMM.2002.800806.

for the derivation is employed that naturally follows from the nonphysical interpretation of the Class-A model introduced in Section II. For this receiver, the upper Chernoff bound on the PEP is derived, and in Section IV-A, the cutoff rates achieved by the suboptimum and optimum decoders are compared. Since the cutoff rate is based on random coding arguments, this analysis is general and does not depend on a particular error-correcting code.

II. Class-A Noise Model

The sender encodes the information by a block code $\mathcal{C}$ with cardinality $|\mathcal{C}|$, codewords $\mathbf{c} = (c_1, \ldots, c_n)$, and code symbols $c_k \in \mathcal{X}$. $\mathcal{X}$ is the set of points of an arbitrary real or complex signal constellation, e.g., the ASK or QAM signal constellation. The bold-faced notation is employed to denote vectors. The c_k's are transmitted over the memoryless AWCN channel. The components of the received vector $\mathbf{r} = (r_1, \ldots, r_n)$ are then given by

$$r_k = c_k + n_k. \tag{1}$$

The n_k's are independently identically distributed (i.i.d.) according to Middleton's Class-A noise model (see [1] and [5]). If the real channel is considered, r_k, c_k, and n_k are real random variables, otherwise they are complex. We use the abbreviation

$$\alpha_m = e^{-A}\frac{A^m}{m!} \tag{2}$$

to write the Class-A probability density function (pdf) for the complex channel

$$p(n_k) = \sum_{m=0}^{\infty} \frac{\alpha_m}{2\pi\sigma_m^2} \exp\left(-\frac{|n_k|^2}{2\sigma_m^2}\right) \tag{3}$$

with the complex valued argument n_k. For the real channel, the pdf is given by

$$p(n_k) = \sum_{m=0}^{\infty} \frac{\alpha_m}{\sqrt{2\pi}\sigma_m} \exp\left(-\frac{n_k^2}{2\sigma_m^2}\right). \tag{4}$$

Note that $p(n_k)$ is the weighted sum of infinitely many Gaussian pdfs with increasing variance

$$\sigma_m^2 = \sigma^2 \frac{m/A + T}{1 + T} \tag{5}$$

where the parameter σ^2 defines the mean variance of the Class-A noise. The Class-A model combines the presence of an additive man-made noise component i_k with average variance σ_i^2 and an AWGN component g_k with variance σ_g^2, i.e., $n_k = i_k + g_k$ holds. The parameter $T = \sigma_g^2/\sigma_i^2$ defines the relative variance of both noise components. The additional AWGN component is introduced in the Class-A model to describe the impact of thermal noise which is naturally present in every real physical receiver. The model's third parameter, A, is called the impulsive index. For small A, say $A = 0.1$, the Class-A noise is highly structured (impulsive) whereas for $A \to \infty$ the pdf becomes Gaussian (see [13]). Finally, the signal-to-noise ratio (SNR) of the AWCN channel is defined as $\mathrm{SNR} := E\{|c_k|^2\}/N_0$, where $E\{\cdot\}$ denotes the expectation operator and $N_0 := 2\sigma^2$ the noise power spectral density.

To gain more insight into the nature of the AWCN channel, we introduce a nonphysical interpretation of this channel employing the terminology of communication theory. Following this approach, each transmitted code symbol c_k is disturbed by AWGN with a pdf $p(n_k \mid m)$. The variance σ_m^2 of this noise is determined by the realization of the random *channel state* $m = 0, 1 \ldots$, using (5). Since the channel is memoryless, the channel states are taken independently with probability $P(m) = \alpha_m$ [see (5)], where $P(m)$ is the Poisson distribution (see [14]), and the capital $P(\cdot)$ is introduced to emphasize that the channel state is a discrete random variable. The channel state is unknown to the observer of the channel output. Hence, the Class-A pdf is given by the expectation over all possible states

$$p(n_k) = \sum_{m=0}^{\infty} \alpha_m p(n_k \mid m).$$

For the complex Class-A distribution, the real and imaginary parts of n_k are statistically dependent. This results from the fact that the real and imaginary components of the complex Gaussian pdf $p(n_k \mid m)$ always have the same variance σ_m^2. In other words, only *one* realization m of the channel state determines the variance of *both* components such that, loosely speaking, the real and imaginary components of the received samples r_k always have the same, but unknown, reliability. In reverse, it can be concluded that the statistical dependence of the real and imaginary components provides the receiver with information about the channel state.

From the nonphysical interpretation of the Class-A process, an algorithm to generate realizations of this process naturally follows. In the first step, the realization of the channel state m is determined. Since α_m tends to zero for increasing m [see (2)], it is sufficient to consider only a finite number of states to achieve a given accuracy. Once m is determined, the noise is generated by the straightforward computation of a Gaussian distributed random variable with variance σ_m^2. The only difficulty of this algorithm is to evaluate realizations of the Poisson distributed random channel state. However, this is relatively simple compared to directly generating the random variable from the continuous Class-A pdf (see [14]).

III. Optimum Reception

A. MAP Decoding Rule

The maximum *a posteriori* (MAP) receiver minimizes the probability of a decoding error (see [15]). It chooses the codeword which maximizes the *a posteriori* probability $P(\mathbf{c} \mid \mathbf{r})$ that the codeword $\mathbf{c}$ was sent given that $\mathbf{r}$ was received. Since the channel is memoryless, it holds that

$$\max_{\mathbf{c}\in\mathcal{C}} P(\mathbf{c} \mid \mathbf{r}) = \max_{\mathbf{c}\in\mathcal{C}} P(\mathbf{c}) \prod_{k=1}^{n} \frac{p(r_k \mid c_k)}{p(r_k)}$$

and, since the noise is additive, it can be written

$$p(r_k \mid c_k) = p(n_k = r_k - c_k).$$

It is assumed that every codeword is sent with equal probability $P(\mathbf{c}) = 1/|\mathcal{C}|$. To simplify the MAP decoding rule, all factors independent of the codeword $\mathbf{c}$ are neglected since they do not affect the maximization. Rewriting the resulting expression in terms of logarithms shows that MAP decoding is equivalent to choosing the codeword which maximizes the additive decoding metric

$$\begin{aligned}\omega(\mathbf{c},\mathbf{r}) &= \sum_{k=1}^{n} \tilde{\omega}(c_k, r_k) \\ &= \sum_{k=1}^{n} \ln p(n_k = r_k - c_k) \\ &= \sum_{k=1}^{n} \ln \sum_{m=0}^{\infty} \frac{\alpha_m}{2\pi\sigma_m^2} \exp\left(-\frac{|c_k - r_k|^2}{2\sigma_m^2}\right) \end{aligned} \quad (6)$$

where the final expression holds for the specific example of the complex AWCN channel. The decoding metric assigns a decision region $\mathcal{D}(\mathbf{c})$ to each codeword $\mathbf{c} \in \mathcal{C}$, i.e.,

$$\mathcal{D}(\mathbf{c}) = \{\mathbf{x} \,|\, \forall \mathbf{c}' \in \mathcal{C},\, \mathbf{c}' \neq \mathbf{c} : \omega(\mathbf{c},\mathbf{x}) > \omega(\mathbf{c}',\mathbf{x})\}. \quad (7)$$

With this region, the MAP decoding rule can be reformulated: given a received vector $\mathbf{r}$, choose the codeword $\mathbf{c}$ for which $\mathbf{r} \in \mathcal{D}(\mathbf{c})$ holds. Given that the codeword $\mathbf{c}$ was transmitted, we denote the probability of a correct decoding result by $P(\mathbf{r} \in \mathcal{D}(\mathbf{c}) \,|\, \mathbf{c})$. Then, the probability of a decoding error for coded transmission immediately follows as

$$P_e = 1 - \frac{1}{|\mathcal{C}|} \sum_{\mathbf{c}\in\mathcal{C}} P(\mathbf{r} \in \mathcal{D}(\mathbf{c}) \,|\, \mathbf{c}). \quad (8)$$

B. Uncoded Transmission

The MAP decoding metric for uncoded transmission is obtained from (6) by setting the codeword length to $n = 1$. This yields

$$\omega(c,r) = \ln \sum_{m=0}^{\infty} \frac{\alpha_m}{2\pi\sigma_m^2} \exp\left(-\frac{|c-r|^2}{2\sigma_m^2}\right)$$

where $c \in \mathcal{X}$ holds since $\mathcal{X}$ and the code $\mathcal{C}$ are identical for $n = 1$. Since for $n = 1$ the codeword and the received vector are scalars, the bold-faced notation for vectors is not used. According to this metric, the receiver chooses the symbol c which has the minimum Euclidean distance to the received symbol r. Hence, the decision regions defined in (7) are equivalent to the decision regions for the AWGN channel (see, e.g., [15]).

Employing (8), the error probability is now calculated as

$$\begin{aligned} P_e &= 1 - \frac{1}{|\mathcal{C}|} \sum_{c\in\mathcal{X}} \int_{\mathcal{D}(c)} p(n_k = x - c)\, dx \\ &= \sum_{m=0}^{\infty} \alpha_m \left[1 - \frac{1}{|\mathcal{C}|} \sum_{c\in\mathcal{X}} \int_{\mathcal{D}(c)} \frac{\exp\left(-\frac{|x-c|^2}{2\sigma_m^2}\right)}{2\pi\sigma_m^2}\, dx\right]. \end{aligned}$$

In this expression, the integrand is the Gaussian distribution with variance σ_m^2. Moreover, as stated above, the decision regions over which we integrate are equivalent to the decision regions of the AWGN channel. Hence, the expression in the square brackets gives the error probability for an uncoded transmission over the AWGN channel with variance σ_m^2. We denote this probability by $P_e^{\mathrm{AWGN}}(\sigma_m^2)$ and get our final result of

$$P_e = \sum_{m=0}^{\infty} \alpha_m P_e^{\mathrm{AWGN}}(\sigma_m^2). \quad (9)$$

This means that, for every uncoded (i.e., memoryless) transmission scheme for which the decoding error probability for the AWGN channel is known, the decoding error probability for the AWCN channel immediately follows from (9). This result holds for the real as well as for the complex channels. In the sense of the state model for Class-A noise (see Section II), the result in (9) can be understood intuitively: since $P_e^{\mathrm{AWGN}}(\sigma_m^2)$ gives the SER achieved if the channel has taken state m, the total SER is simply given by the expected value over all channel states.

C. Coded Transmission and Chernoff Bound

In the case of coded transmission, the evaluation of the exact error probability given by (8) is very difficult. Therefore, the union bound is used to obtain an asymptotically tight upper bound

$$P_e \leq \frac{1}{|\mathcal{C}|} \sum_{\mathbf{c}\in\mathcal{C}} \sum_{\mathbf{c}'\in\mathcal{C},\, \mathbf{c}'\neq\mathbf{c}} P(\mathbf{c} \to \mathbf{c}')$$

where $P(\mathbf{c} \to \mathbf{c}')$ is the pairwise error probability (PEP), i.e., the probability that in the binary decision between $\mathbf{c}$ and $\mathbf{c}'$ the decoder erroneously decodes $\mathbf{c}' \neq \mathbf{c}$ given that $\mathbf{c}$ was transmitted (see [15]). Defining $\Omega := \omega(\mathbf{c}',\mathbf{r}) - \omega(\mathbf{c},\mathbf{r})$, the PEP is given by

$$P(\mathbf{c} \to \mathbf{c}') = P(\Omega > 0 \,|\, \mathbf{c}) = \int_0^{\infty} p(\Omega = x \,|\, \mathbf{c})\, dx.$$

Since $\omega(\mathbf{c},\mathbf{r})$ is an additive decoding metric, the Chernoff bounding technique yields

$$P(\mathbf{c} \to \mathbf{c}') \leq \min_{\lambda} \prod_{k=1}^{n} C(c_k, c_k', \lambda) \quad (10)$$

(see [15]) with the Chernoff factors

$$C(c_k, c_k', \lambda) = \int_{-\infty}^{\infty} e^{\lambda(\tilde{\omega}(c_k', r_k) - \tilde{\omega}(c_k, r_k))} p(r_k \,|\, c_k)\, dr_k \quad (11)$$

where this integration is one-dimensional (1-D) for the real and two-dimensional (2-D) for the complex channel. The parameter $\lambda \geq 0$ is used to minimize the bound, and since the channel noise is additive [see (1)], $p(r_k \,|\, c_k) = p(n_k = r_k - c_k)$ holds. If MAP detection is used, $\lambda = (1/2)$ minimizes the Chernoff factor and the bound in (10) can be tightened by a factor of $(1/2)$ (see [12]). With this we obtain

$$\min_{\lambda} C(c_k, c_k', \lambda) = \int_{-\infty}^{\infty} \sqrt{p(n_k = x - c_k) p(n_k = x - c_k')}\, dx.$$

The Chernoff factor $C(c_k, c_k', \lambda = (1/2))$ only depends on the Euclidean distance $d_k := |c_k - c_k'|$ between the code symbols c_k and c_k'. Therefore, the abbreviation

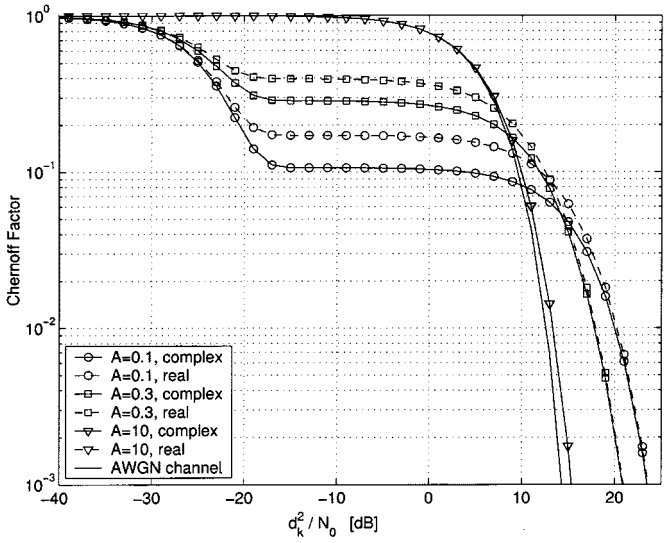

Fig. 1. Chernoff factors for the real and complex channels with $T = 10^{-3}$, various parameters A, and MAP decoding.

$C(d_k) := \min_\lambda C(c_k, c_k', \lambda)$ is introduced which yields the final result for the complex channel

$$C_{\text{compl}}^{\text{MAP}}(d_k) = \frac{1}{2\pi} \int \int_{-\infty}^{\infty} \sqrt{\sum_{m=0}^{\infty} \frac{\alpha_m}{\sigma_m^2} e^{-\frac{(x-d_k/2)^2+y^2}{2\sigma_m^2}}} \times \sqrt{\sum_{m=0}^{\infty} \frac{\alpha_m}{\sigma_m^2} e^{-\frac{(x+d_k/2)^2+y^2}{2\sigma_m^2}}}\, dx\, dy. \quad (12)$$

The above expression is a straightforward extension of the Chernoff factor for the real channel (see [13])

$$C_{\text{real}}^{\text{MAP}}(d_k) = \frac{1}{\sqrt{2\pi}} \int_{-\infty}^{\infty} \sqrt{\sum_{m=0}^{\infty} \frac{\alpha_m}{\sigma_m} e^{-\frac{(x-d_k/2)^2}{2\sigma_m^2}}} \times \sqrt{\sum_{m=0}^{\infty} \frac{\alpha_m}{\sigma_m} e^{-\frac{(x+d_k/2)^2}{2\sigma_m^2}}}\, dx. \quad (13)$$

Although both factors are functions of d_k and the noise variance σ^2, it can be shown that they actually depend on the ratio $d_k^2/(2\sigma^2) = d_k^2/N_0$ only.

In Fig. 1, $C_{\text{compl}}^{\text{MAP}}(d_k)$ and $C_{\text{real}}^{\text{MAP}}(d_k)$ are plotted for $T = 10^{-3}$ and various different values of A. Additionally, the Chernoff factor for the AWGN channel

$$C_{\text{AWGN}}(d_k) = \exp\left(-\frac{d_k^2}{8\sigma^2}\right) \quad (14)$$

(see [15]) is depicted. For $A = 10$, the curves for the real and the complex channels are similar and almost match the bound for the AWGN channel. The behavior is in agreement with the fact that for large A the channel converges to the AWGN channel (see [5]). As A becomes smaller, i.e., the noise becomes more impulsive, the curves for the complex channel show a better performance, especially in the region of the error floor. This behavior could be expected since, for the complex channel, the decoder can exploit the additional channel state information provided by the statistical dependence of the real and imaginary components of the complex Class-A distribution (see Section II).

IV. Suboptimum Reception

The calculation of the MAP decoding metric [see (6)] is quite complicated. To obtain a simpler receiver, a suboptimum decoding metric with lower complexity is derived in this section. In the following, only the complex AWCN channel is considered since the results for the real channel are similar.

The starting point of the derivation is the state model for AWCN channel (see Section II). The suboptimum receiver jointly estimates the codeword $\mathbf{c}$ and the channel state vector $\mathbf{m} = (m_1, \ldots, m_n)$, where m_k is the channel state while transmitting the code symbol $c_k \in \mathcal{X}$. Employing the MAP estimation rule for the joint estimator yields

$$\max_{\mathbf{m},\mathbf{c}} P(\mathbf{c}, \mathbf{m} \,|\, \mathbf{r}) = \max_{\mathbf{c} \in \mathcal{C}} P(\mathbf{c}) \prod_{k=1}^{n} \max_{m_k} \frac{p(r_k \,|\, c_k, m_k) P(m_k)}{p(r_k)}$$

where $P(\mathbf{c}, \mathbf{m} \,|\, \mathbf{r})$ is the probability that, given that $\mathbf{r}$ was received, the channel states are given by $\mathbf{m}$ and the codeword $\mathbf{c} \in \mathcal{C}$ was transmitted. The pdf $p(r_k \,|\, c_k, m_k)$ is Gaussian with mean c_k and variance $\sigma_{m_k}^2$, and $P(m_k) = \alpha_{m_k}$ is the probability that the channel is in state m_k [see (2)]. Since infinitely many states m_k exist, we restrict the number of states considered for the maximization to $m_k = 0, \ldots, L$. This corresponds to a truncation of the infinite sum in the Class-A pdf [see (3)], after $L+1$ terms. Following the procedure described in Section III-A, the suboptimum decoding metric is finally obtained as

$$\begin{aligned} \varphi(\mathbf{c}, \mathbf{r}) &= \sum_{k=1}^{n} \ln \max_{m_k = 0, \ldots L} \alpha_{m_k} p(r_k \,|\, c_k, m_k) \\ &= \sum_{k=1}^{n} \max_{m_k = 0, \ldots L} \left\{ \ln\left(\frac{\alpha_{m_k}}{\sigma_{m_k}^2}\right) - \frac{|r_k - c_k|^2}{2\sigma_{m_k}^2} \right\}. \end{aligned}$$

Note that for $L = 0$ this metric is equivalent to the MAP decoding metric for the AWGN channel (see [15]), since, for $L = 0$, several terms independent of the codeword can be cancelled.

Comparing the complexity of the MAP decoding metric $\omega(\mathbf{c}, \mathbf{r})$ [see (6)] and the suboptimum metric $\varphi(\mathbf{c}, \mathbf{r})$ is not directly possible since calculating $\omega(\mathbf{c}, \mathbf{r})$ requires the evaluation of an infinite sum which is not possible in the practical situation. Therefore, to simplify the complexity comparison, we assume that the sum in (6) is also truncated after the Lth term. Then, to calculate $\omega(\mathbf{c}, \mathbf{r})$, one evaluation of $\ln(\cdot)$ and $L+1$ evaluations of $\exp(\cdot)$ are required for each received sample r_k. In contrast, for the suboptimum metric, these operations are not required: since the $\ln(\cdot)$ terms are independent of the received sample, they can be precomputed and included in the metric calculation using a fast table-lookup operation.

It is interesting to note that, based on an approximation of the Class-A pdf, in [7] and [8] the same metric $\varphi(\mathbf{c}, \mathbf{r})$ was derived for the special case $L = 2$. However, the receiver is not compared to the MAP decoder and analyzed using simulation results only.

For uncoded transmission, the suboptimum decoder is equivalent to the MAP decoder and its performance is there-

fore also given by (9). To obtain a performance measure for coded transmission, the Chernoff factors for the suboptimum decoding metric are derived following the same procedure as in Section III-C. Again, the factors only depend on the Euclidean distance $d_k = |c_k - c'_k|$ between the code symbols, so we obtain

$$C_{\text{compl}}^{\text{sub}}(d_k,\lambda) = \sum_{m=0}^{\infty} \frac{\alpha_m}{2\pi\sigma_m^2} \int\int e^{-\frac{(x-\frac{1}{2}d_k)^2+y^2}{2\sigma_m^2}} \times \max_{l=0,\ldots,L} \left\{ \frac{\alpha_l}{\sigma_l^2} e^{-\frac{(x+\frac{1}{2}d_k)^2+y^2}{2\sigma_l^2}} \right\}^{\lambda} \times \max_{j=0,\ldots,L} \left\{ \frac{\alpha_j}{\sigma_j^2} e^{-\frac{(x-\frac{1}{2}d_k)^2+y^2}{2\sigma_j^2}} \right\}^{-\lambda} dx\,dy \tag{15}$$

with the parameter $\lambda \geq 0$. If the MAP decoding metric for the AWGN channel is employed, i.e., $L = 0$ holds, the integral can be solved analytically.

Numerical investigations show that the optimal choice of λ depends on the distance d_k. This means that the min-operator and the product in (10) cannot be exchanged. Therefore, a comparison of the Chernoff factors for optimum and suboptimum reception is not useful since the best choice of λ for the suboptimum reception always depends on the particular codewords and the signal constellation $\mathcal{X}$ adopted. To overcome this problem, in the next section, both receivers are compared employing the cutoff rate as a performance criterion.

A. Cutoff Rate

The cutoff rate R_0 is derived based on random coding arguments and provides a general performance measure similar to the channel capacity [3]. We define R as the average number of information bits transmitted per channel use. Then, it can be shown that, for any code length n, a code with $R < R_0$ exists such that for its decoding error probability the following holds [3]:

$$P_e < e^{-n(R_0-R)}.$$

The formula shows that, for any $R < R_0$, an arbitrarily small decoding error probability can be achieved by increasing n.

Employing the Chernoff factors derived in the previous section, the cutoff rates can be calculated easily using the relation

$$R_0 = -\log_2 \min_{\lambda} \sum_{x\in\mathcal{X}} \sum_{y\in\mathcal{X}} P(x)\,P(y)\,C(x,y,\lambda) \tag{16}$$

see [11], [12], where $P(x)$ and $P(y)$ are the probabilities that the symbols x and y from the channel input alphabet $\mathcal{X}$ are transmitted respectively. For our analysis, it is assumed that every symbol of $\mathcal{X}$ is equally likely to be transmitted, i.e., $P(x) = P(y) = 1/|\mathcal{X}|$. For MAP decoding, it was already discussed in the previous section that the Chernoff factors

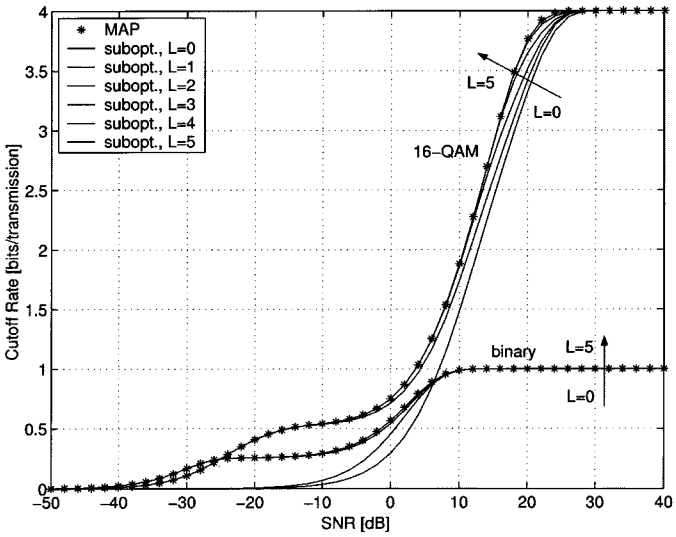

Fig. 2. Cutoff rates for the complex AWCN channel ($A = 1, T = 10^{-3}$) adopting binary and 16-QAM modulation with MAP and suboptimum decoding.

$C(x,y,\lambda)$ are minimized by $\lambda = 1/2$ so the expression for the cutoff rate reduces to

$$R_0^{\text{MAP}} = -\log_2 \frac{1}{|\mathcal{X}|^2} \sum_{x\in\mathcal{X}} \sum_{y\in\mathcal{X}} C^{\text{MAP}}(d_k)$$

where $C^{\text{MAP}}(\cdot)$ is given by (12), (13), and $d_k := |x-y|$. However, for suboptimum reception, the sum and the min-operator cannot be exchanged in (16) since the optimum choice of λ depends on the distance d_k. Hence, the cutoff rate of the suboptimum decoder is given by

$$R_0^{\text{sub}} = -\log_2 \frac{1}{|\mathcal{X}|^2} \min_{\lambda} \sum_{x\in\mathcal{X}} \sum_{y\in\mathcal{X}} C^{\text{sub}}(d_k,\lambda).$$

Since the formulas for R_0^{MAP} and R_0^{sub} are very complicated, both expressions are compared employing numerical methods. The minimization operator in the expression for R_0^{sub} is evaluated by an iterative algorithm. Since in the SNR region under investigation the Chernoff factors are observed to strongly grow for $\lambda > 1$ and increasing λ, the iterative minimization procedure operates on the interval $0 \leq \lambda \leq 1$. The first estimate for minimizing λ is determined by exhaustively searching though the interval $0 \leq \lambda \leq 1$ with a step size of $\Delta^{(1)} = 10^{-3}$. In the interval $\pm\Delta^{(1)}$ around the located minimum, the exhaustive search is then repeated with the reduced step size $\Delta^{(2)} = \Delta^{(1)}/10$. This procedure is repeated until the cutoff rate $R_0^{\text{sub},(k)}$, evaluated in the kth iteration, fulfills the stop criterion $|R_0^{\text{sub},(k)} - R_0^{\text{sub},(k-1)}| < 10^{-4}$. For almost all cases, the minimum found in the first iteration could not be significantly improved by decreasing the step size. Hence, the initial step size $\Delta^{(1)} = 10^{-3}$ seems to be sufficient to find the global minimum in the interval $0 \leq \lambda \leq 1$. Although this is no strict mathematical proof, from our investigations we conclude that numerically solving the minimization operator is not critical and the algorithm indeed finds the global minimum.

In Fig. 2, the cutoff rates for optimum and suboptimum decoding are depicted for the example of the complex AWCN

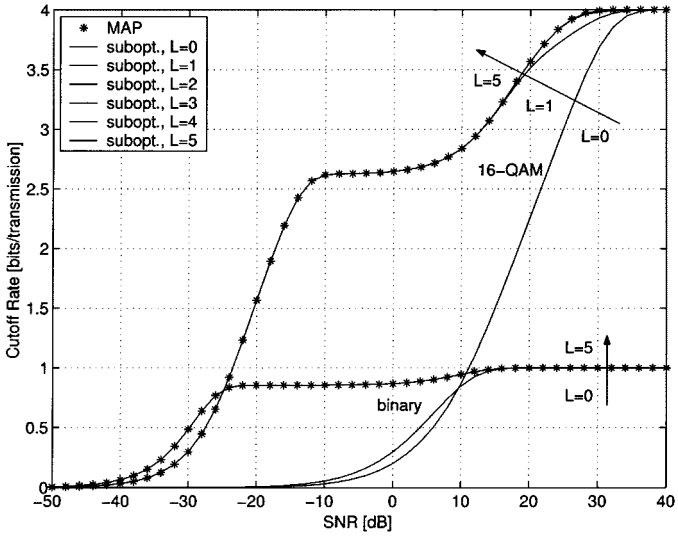

Fig. 3. Cutoff rates for the complex AWCN channel ($A = 0.1, T = 10^{-3}$) adopting binary and 16-QAM modulation with MAP and suboptimum decoding.

TABLE I
PERFORMANCE OF THE SUBOPTIMUM DECODER ON THE AWCN CHANNEL ADOPTING QAM MODULATION

A	T	QAM	L	ΔR_0 for $L \to \infty$
0.1; 0.3	10^{-3}	16	2; 3	0.03%; 0.12%
0.6; 1.0	10^{-3}	16	3; 4	0.25%; 0.40%
0.1; 1.0	10^{-2}	16	2; 4	0.04%; 0.49%
0.1; 1.0	1	16	2; -	0.98%; 2.85%
0.1; 1.0	10^{-3}	4	1; 2	0.02%; 0.25%
0.1; 1.0	1	4	1; -	0.78%; 2.20%

channel with parameters $A = 1, T = 10^{-3}$. Both binary and 16-QAM modulation are considered. For the conventional AWGN receiver (i.e., $L = 0$), especially in the low SNR region, a large divergence between the optimum and suboptimum decoder can be observed. However, for binary modulation, already for $L = 1$, the suboptimum decoder almost achieves the performance of MAP decoding. In contrast, for 16-QAM and the worst case SNR, a value of $L \geq 4$ is required. For other SNR values, typically smaller L values are sufficient.

Fig. 3 shows the cutoff rates for the complex AWCN channel with parameters $A = 0.1$ and $T = 10^{-3}$. In contrast to the example discussed previously, the performance degradation when employing the conventional AWGN receiver ($L = 0$) is larger. This could be expected since for smaller A the AWCN channel becomes more impulsive. Additionally, it can be observed that, compared to the case $A = 1$, for both modulation schemes, smaller L values are sufficient to almost achieve the performance of the MAP decoder. This shows that the performance of the suboptimum decoder depends on the channel parameters.

From the figures, it seems that the suboptimum decoder achieves the performance of MAP decoding if L is chosen large enough. Therefore, the relative difference

$$\Delta R_0 = \left(R_0^{\mathrm{MAP}} - R_0^{\mathrm{sub}}\right) / R_0^{\mathrm{MAP}}$$

has been further analyzed for the channels with all possible combinations of the parameters $A \in \{0.1; 0.3; 0.6; 1\}, T \in \{10^{-3}; 10^{-2}; 10^{-1}; 1\}$, 4-QAM and 16-QAM modulation. For the numerical study, the SNR values from -30 to 40 dB were investigated with a step size of 2 dB. For all examples, it could be observed that at a certain point a further increase of L could not further reduce ΔR_0. Hence, even for $L \to \infty$, the suboptimum decoder cannot achieve the performance given by MAP decoding. We conclude that, for small L, the decoder's performance is mainly limited by the truncation of the Class-A pdf to $L + 1$ terms, whereas, for larger L, the degradation is caused by the suboptimum estimation criterion employed to derive $\varphi(\mathbf{c}, \mathbf{r})$.

In Table I, some numerical results are summarized. The fifth column gives the remaining ΔR_0 that could not be removed by increasing L. In the fourth column, the L value required to achieve a relative difference $\Delta R_0 < 2\%$ is given. The idea behind choosing $\Delta R_0 < 2\%$ is that such a small value is typically negligible in the practical situation, and therefore the performance of MAP decoding is practically achieved. Note that ΔR_0 is actually a function of the SNR. In the table, the worst case SNR is considered that typically lies in the region where the cutoff rate approaches its maximum (see Fig. 2).

The table shows that an increase of A, T or the size of the QAM modulation alphabet decreases the performance of the suboptimum receiver. Particularly if both A and T are large, the performance significantly degrades as illustrated by the two cases in Table I for which $\Delta R_0 < 2\%$ could not be achieved. However, for both cases, a difference $\Delta R_0 \leq 3\%$ could already be achieved using $L = 4$. Hence, we conclude that for channel parameters of $A \leq 1$ and $T \leq 1$ and modulation schemes up to 16-QAM the suboptimum decoder shows an excellent performance while providing a lower complexity than the MAP decoder. In all other cases, no general statements are possible and the decoders performance must be analyzed separately.

V. CONCLUSION

The interpretation of the Class-A random process using a state model is useful to gain more insight into the nature of the AWCN channel. It not only leads to a low-complexity algorithm to generate realizations of Class-A distributed random variables, but also enables an intuitive interpretation of the results obtained in this paper.

The first part of the paper addresses the transmission over the AWCN channel using MAP decoding. We show that the SER for uncoded transmission is obtained by averaging over the SER obtained for each channel state. Therefore, a simple relation between the SER of the AWCN and the AWGN channel exists. The analysis of the Chernoff factors for the real and complex AWCN channel shows that the complex channel is superior over the real channel in terms of the achievable SER. Loosely speaking, for the complex channel, the receiver can use the information that the noise on the real and the imaginary components originated from the same channel state.

The derivation of a low-complexity suboptimum receiver using the state model for the Class-A noise is given in the second part of the paper. The performance analysis using the cutoff rate shows that, for small L, the truncation of the infinite sum-term in the Class-A pdf and, for large L, the suboptimum

design criteria limit the performance of the suboptimum decoder. The number of states L employed by the suboptimum decoder should be adapted to the modulation scheme, the SNR, and the parameters A, T. However, for $A \leq 1, T \leq 1$ and schemes up to 16-QAM, a value of $L = 4$ is sufficient to keep the relative difference over MAP decoding ΔR_0 below 3%.

REFERENCES

[1] L. A. Berry, "Understanding Middleton's canonical formula for class-A noise," *IEEE Trans. Electromagn. Compat.*, vol. EMC-23, pp. 337–344, Nov. 1981.

[2] P. A. Delaney, "Signal detection in multivariate class A interference," *IEEE Trans. Commun.*, vol. 43, pp. 365–373, Feb./Mar./Apr. 1995.

[3] R. G. Gallager, *Information Theory and Reliable Communication*. New York: Wiley, 1968.

[4] K. F. McDonald and R. S. Blum, "A statistical and physical-mechanisms based interference and noise model for antenna array observations," *IEEE Trans. Signal Processing*, vol. 48, pp. 2044–2056, July 2000.

[5] D. Middleton, "Canonical and quasicanonical probability models of class A interference," *IEEE Trans. Electromagn. Compat.*, vol. EMC-25, pp. 76–106, May 1983.

[6] ——, "Procedures for determining the parameters of the first-order canonical models of class A and Class B electromagnetic interference," *IEEE Trans. Electromagn. Compat.*, vol. EMC-21, pp. 190–208, Aug. 1979.

[7] S. Miyamoto, M. Katayama, and N. Morinaga, "Performance analysis of QAM systems under class A impulsive noise environment," *IEEE Trans. Electromagn. Compat.*, vol. 37, pp. 260–267, May 1995.

[8] S. Miyamoto and N. Morinaga, "Signal-detection characteristics in Trellis-coded modulation system under impulsive noise environment and its optimum reception," *Trans. IEICE*, vol. J75-B-II, no. 10, pp. 671–681, Oct. 1992.

[9] R. Prasad, A. Kegel, and A. de Vos, "Performance of microcellular mobile radio in a cochannel interference, natural, and man-mande noise environment," *IEEE Trans. Veh. Technol.*, vol. 42, pp. 33–39, Feb. 1993.

[10] J. Proakis, *Digital Communications*, 3rd ed. New York: McGraw-Hill, 1995.

[11] C. Schlegel and D. J. Costello, "Bandwidth efficient coding for fading channels: Code construction and performance analysis," *IEEE J. Select. Areas Commun.*, vol. 7, Dec. 1989.

[12] M. Simon, J. Omura, R. Scholz, and B. Levitt, *Spread Spectrum Communications*. Rockville, MD: Computer Science Press, 1985, vol. I.

[13] A. D. Spaulding and D. Middleton, "Optimum reception in an impulsive interference environment—Part I: Coherent detection," *IEEE Trans. Commun.*, vol. COM-25, pp. 910–923, Sept. 1977.

[14] W. H. Press *et al.*, *Numerical Recipes in C: The Art of Scientific Computing*, 2nd ed. Cambridge, U.K.: Cambridge Univ. Press, 1993.

[15] J. M. Wozencraft and M. Jacobs, *Principles of Communication Engineering*. New York: Wiley, 1965.

[16] S. M. Zabin and H. V. Poor, "Parameter estimation for middleton class-A interference processes," *IEEE Trans. Commun.*, vol. 37, pp. 1042–1051, Oct. 1989.

Jürgen Häring received the diploma in electrical engineering from the University of Dortmund, Germany, in 1998 and the Ph.D. degree from the Institute for Experimental Mathematics, University of Essen, Germany, in 2001.

In 2002, he joined the digital signal processing group at Tesat-Spacecom, Germany, where he develops on-board signal processing systems for satellites. His research interests include coding and modulation for fading and impulsive noise channels, powerline communications, satellite communications, and information theory.

A. J. Han Vinck (M'77–SM'91) received the Ph.D. degree in electrical engineering from the University of Eindhoven, The Netherlands in 1980.

He has been a Full Professor in Digital Communications at the University of Essen, Essen, Germany, since 1990. His interests is in information and communication theory, coding and network aspects in digital communications. From 1991 to 1993 and 1998 to 2000, he was the director of the Institute for Experimental Mathematics in Essen.

Prof. Vinck has served on the Board of Governors of the IEEE Information Theory Society since 1997 (until 2003). In 2001, he was elected 1st Vice President of the IEEE Information Theory Society. In 1999, he was the Program Chairman for the IEEE IT workshop in Kruger Park, South Africa, and in 1997 he acted as Co-chairman for the 1997 IEEE Information Theory Symposium in Ulm, Germany (704 participants). He was founding Chairman (1995–1998) of the IEEE German Information Theory chapter. In 1990 he organized the IEEE Information Theory Workshop in Veldhoven, The Netherlands. He is the initiator of the Japanese-Benelux workshops on information theory and the international winter meeting on coding, cryptography and information theory. He is a driving force behind the organization of the series of conferences on Power Line Communications and its Applications (ISPLC). In 1998 he was elected chairman of the Benelux Information and Communication Theory Society.